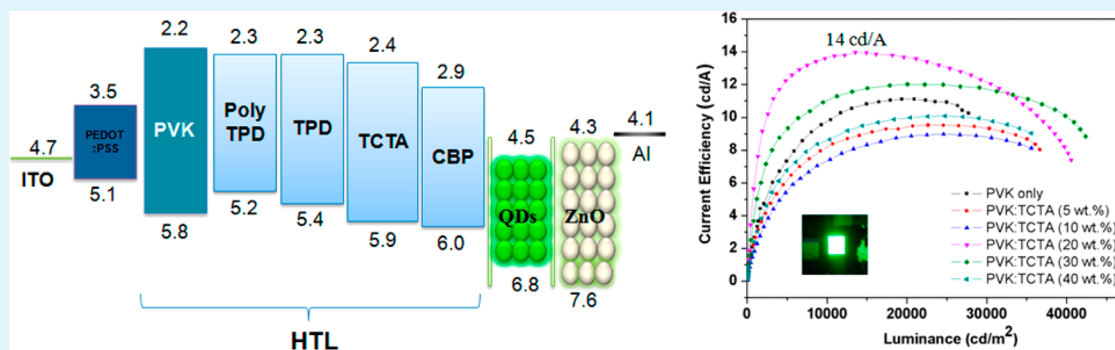


Polymer and Small Molecule Mixture for Organic Hole Transport Layers in Quantum Dot Light-Emitting Diodes

My Duyen Ho,[†] Daekyoung Kim,[†] Namhun Kim,[†] Sung Min Cho,[†] and Heeyeop Chae^{*,†,‡}

[†]School of Chemical Engineering, Sungkyunkwan University, Suwon 440-746, South Korea

[‡]Sungkyunkwan Advanced Institute of Nanotechnology, Sungkyunkwan University, Suwon 440-746, South Korea



ABSTRACT: The performance of quantum dot light-emitting diodes (QD-LEDs) was investigated for different hole transport layers with small molecules and polymers: poly(4-butyl-phenyl-diphenyl-amine), poly-*N*-vinylcarbazole (PVK), *N,N'*-diphenyl-*N,N'*-bis(3-methylphenyl)-1,1'-diphenyl-4,4'-diamine, 4,4',4''-tris(*N*-carbazolyl)-triphenyl-amine (TCTA), and 4,4'-bis-(carbazole-9-yl)biphenyl (CBP). The electroluminescence performance of QD-LEDs was considerably improved by adding small molecules (TCTA or CBP) having high hole mobility to the polymer hole transport material (PVK). The maximal current efficiency of QD-LED-based PVK was improved by 27% upon addition of 20 wt % TCTA due to the hole injection improvement. The lower turn-on voltage, the higher current density, and the higher luminance were achieved by addition of TCTA. The maximal luminance of 40900 cd/m² and the highest current efficiency of 14.0 cd/A with the narrow full width at half-maximum (<35 nm) were achieved by the best hole transport layer.

KEYWORDS: hole transport materials, hole transport, HTL, quantum dot, QD, QLED, QD-LED

1. INTRODUCTION

Quantum dots (QDs) are considered as promising light-emitting materials because of their high color purity, tunable band gaps, photostability, and solution processability.^{1–5} QDs bring the unique benefits of a high color rendering index (CRI) and a broad color gamut, which are required for next-generation display devices.⁶ Recent reports show the importance of charge transport layers. Recent improvements in the brightness and efficiency of QD-LED devices are attributed to the adoption of metal oxide nanoparticles as the electron transport layer (ETL). Several metal oxides, including tin oxide (SnO₂), zinc oxide (ZnO), zinc tin oxide (ZTO),^{7,8} and titanium oxide (TiO₂),⁹ have been reported as the ETL, which maintain the carrier injection balance. Among them, ZnO nanoparticles have allowed QD-LEDs to have the highest brightness and efficiency. Qian et al. reported up to 4200 cd/m² brightness and 0.22% external quantum efficiency (EQE) for blue emission, 68000 cd/m² brightness and 1.8% EQE for green, and 31000 cd/m² brightness and 1.7% EQE for orange-red QD-LEDs with ZnO nanoparticles being adopted as the ETL.¹⁰ Kwak et al. also demonstrated bright QD-LEDs with ZnO nanoparticles in an inverted layer structure, revealing maximal luminance of 23040, 218800, and 2250 cd/m² and EQE values of 7.3, 5.8, and 1.7%

for red, green, and blue, respectively.¹¹ With regard to hole transport, it is known that a large charge barrier of the highest occupied molecular orbital (HOMO) level exists between the hole transport layer (HTL) and the QD light-emitting layer. Typically, the valence bands of QDs are below -6.0 eV, while the HOMO energy levels of common organic semiconductors are located around -5.0 eV. Therefore, the charge injection from the HTL into the QD layer is limited compared to that of a conventional OLED, resulting in more unbalanced hole–electron recombination. To overcome this crucial challenge, metal oxides (NiO and WO₃) with rather low HOMO levels (from -5.5 to -6.3 eV) have been utilized as HTLs.^{7,8,12} However, QD-LEDs based on sputtered metal oxide HTLs were reported to have much poorer performance than devices based on organic HTLs.⁸ Various processes have been proposed to form the HTL. Phase separation of HTL and QD materials was proposed to deposit HTL and QD layers at the same time from a HTL and QD mixture.¹³ Thermal polymerization was also suggested to form the HTL.^{14,15} However,

Received: August 1, 2013

Accepted: October 1, 2013

Published: October 1, 2013

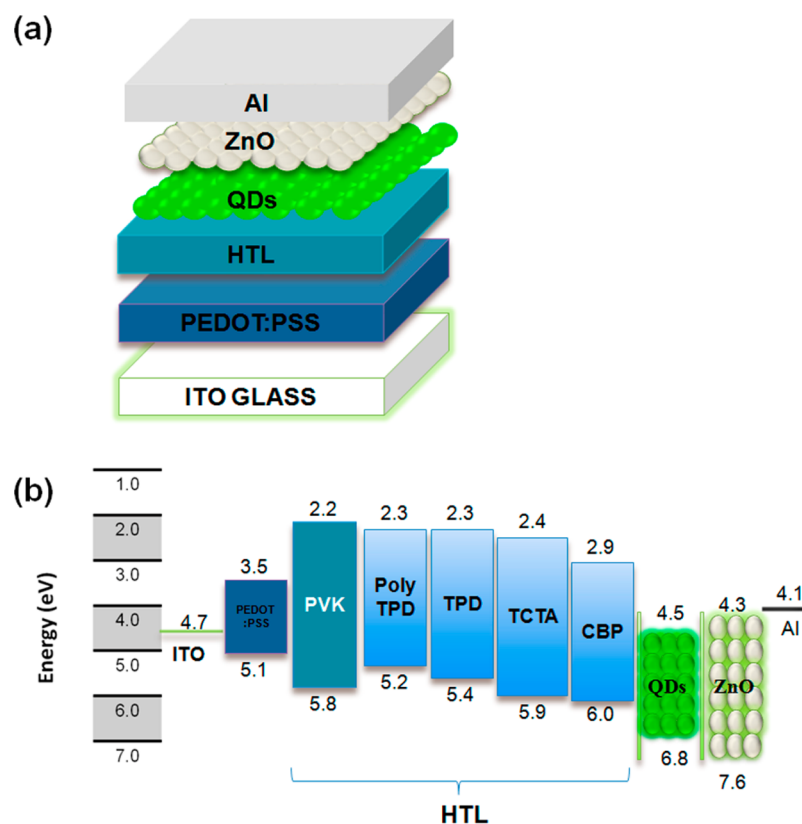


Figure 1. (a) Schematic of the device structure (ITO/PEDOT/HTL/QDs/ZnO/Al). (b) Energy diagram of materials used in this study.

the spin-coating of organic polymer materials is the most popular process for HTL formation. In this work, we investigated polymers, small molecules, and their compositions for the formation of HTLs by the spin-coating process.

2. EXPERIMENTAL SECTION

2.1. Synthesis of Alloyed CdSeZnS QDs with a Chemical Composition Gradient and ZnO Nanoparticles. 2.1.1. Chemicals.

All reagents used in this study were purchased at analytical reagent grade and used for synthesis without further purification. Cadmium oxide (CdO, 99.9%), zinc acetate [$\text{Zn}(\text{acet})_2$, 99.99%], selenium (Se, 99.9%), sulfur (S, 99.9%), oleic acid (OA, 90%), 1-octadecene (ODE, 90%), trioctylphosphine (TOP, 90%), dimethyl sulfoxide (DMSO, HPLC grade, 99.7%), tetramethylammonium hydroxide (TMAH, 97%), hexane (HPLC grade, 97.0%), and ethanol (ACS grade, 99.5%) were purchased from Sigma-Aldrich. Acetone (99.5%) was obtained from Daejung Chemicals and Metals Co., Ltd.

2.1.2. Synthesis of Alloyed CdSeZnS QDs with a Chemical Composition Gradient. Green CdSeZnS QDs were synthesized on the basis of a method reported by Bae et al.¹⁶ CdO, $\text{Zn}(\text{acet})_2$, and OA were placed in a flask, stirred, heated to 150 °C, and degassed for 30 min. Following the addition of ODE, the solution was heated to 310 °C. At this temperature, a stock solution of Se and S in TOP was quickly injected into the heated solution. The reaction temperature was kept at 300 °C for 10 min. The green CdSeZnS QDs were passivated by aliphatic ligands. Then the reaction solution was cooled to room temperature and purified with hexane and excess ethanol by centrifugation. Finally, the precipitate was dispersed in hexane for optical characterization and device fabrication steps.

2.1.3. Synthesis of ZnO Nanoparticles. ZnO nanoparticles were synthesized for the electron transport layer (ETL). The synthesis process for ZnO nanoparticles 5 nm in diameter was as follows. $\text{Zn}(\text{acet})_2$ in a DMSO solution and TMAH in an ethanol solution were stirred for 1 h under ambient conditions and then washed with

ethanol and an excess acetone mixture. Finally, ZnO nanoparticles were dispersed in ethanol to obtain a 30 mg/mL stock solution.¹⁰

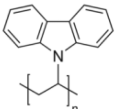
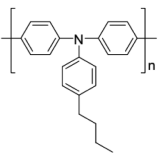
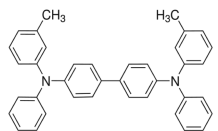
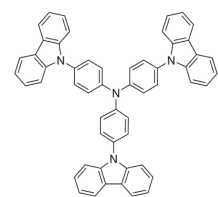
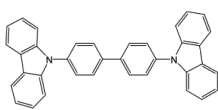
2.1.4. Characterization. UV-vis absorption and photoluminescent (PL) spectra were recorded with an FP-6200 spectrofluorometer and a V-630 Bio UV-vis spectrophotometer, respectively. The transmission electron microscope (TEM) images of the QDs were obtained using a JEM ARM 200F instrument at 20 kV to analyze their average size and size distribution. The fluorescent quantum yield (QY) of the QDs prepared was measured and estimated by using Rhodamine 6G as a standard dye (Rhodamine 6G dissolved in ethanol, QY of 95%) following the relative method^{17,18} under ambient conditions. In this case, the QY can be calculated using the equation

$$Q = Q_R \left(\frac{I}{I_R} \right) \left(\frac{\text{OD}_R}{\text{OD}} \right) \left(\frac{n^2}{n_R^2} \right)$$

where Q is the fluorescence quantum yield, I is the integrated fluorescence intensity, n is the refractive index of solvent, and OD is the optical density (absorption). The subscript R refers to the parameters of the reference.

2.2. Device Fabrication and Characterizations. The QD-LED device adopted the following conventional multilayer structure: ITO/PEDOT:PSS [poly(ethylenedioxythiophene):polystyrene sulfonate, 35 nm]/various HTLs (20–40 nm)/green CdSeZnS QDs (25 nm)/ZnO nanoparticle layer (40 nm)/Al (100 nm), as shown in Figure 1. The ITO glass substrates were cleaned with deionized water, 2-propanol, and acetone. Then these substrates were treated under UV ozone. All HTL, emitting layer (EML), and ETL layers were prepared by the spin-coating process. The PEDOT:PSS layers were spin-coated onto the ITO glass substrates at 4000 rpm for 30 s and baked at 120 °C for 15 min under ambient conditions. In the next step, the samples were transferred to a glovebox for deposition of the additional layers. Various HTL materials were spin-coated and baked: small molecule (in 1,2-dichloroethane) HTL materials were baked at 80 °C and polymer (in chlorobenzene) HTL materials at 120 °C. The effects of various organic hole transport materials, including poly(4-butyl-phenyl-diphenyl-amine)

Table 1. Properties of Different Hole Transport Materials Used in This Study

Hole material	Structure	HOMO (eV)	LUMO (eV)	Hole mobilities (cm ² /V.s)
PVK		5.8	2.2	2.5 × 10 ⁻⁶ (Ref. 23)
Poly-TPD		5.2	2.3	1.0 × 10 ⁻⁴ (Ref. 26)
TPD		5.5	2.3	1.1 × 10 ⁻³ (Ref. 23,24)
TCTA		5.7	2.4	2.0 × 10 ⁻⁵ (Ref. 23,24)
CBP		6.0	2.9	1.0 × 10 ⁻³ (Ref. 11,24)

(poly-TPD), poly-*N*-vinylcarbazole (PVK), *N,N'*-diphenyl-*N,N'*-bis(3-methylphenyl)-1,1'-diphenyl-4,4'-diamine (TPD), 4,4',4''-tris(*N*-carbazolyl)-triphenyl-amine (TCTA), and 4,4'-bis(carbazole-9-yl)-biphenyl (CBP), on the brightness and efficiency of QD-LED were investigated. In the next step, QDs in hexane were spin-coated and ZnO nanoparticles were also spin-coated on top of the QD emitting layer. The samples were baked at 150 °C. Finally, the aluminum cathode was thermally evaporated on top of the ZnO nanoparticle layer at a pressure of 5×10^{-6} Torr.

All electrical measurements were performed under ambient conditions. Luminescence (*L*), current (*I*), and voltage (*V*) characteristics were analyzed with a source measure unit (2400, Keithley Instruments, Inc., Cleveland, OH) and a luminance meter (CS100, Konica Minolta Sensing, Inc., Sakai, Osaka, Japan). EL characteristics were determined using Ocean Optics spectrometers (Ocean Optics Inc.).

3. RESULTS AND DISCUSSION

3.1. Effects of Small Molecules and Polymer-Based HTLs on QD-LEDs. Various small molecules and polymer materials were investigated as hole transport materials for QD-LEDs, including TPD, CBP, poly-TPD, and PVK.^{11,13,19–21} These materials are widely used as materials for HTLs of QD-LEDs; however, a comparative study of the properties of these hole transport materials and their effects on the performances of QD-LEDs has yet to be reported. The molecular structures, band gap levels, and hole mobilities of the hole transport materials utilized in this study are summarized in Table 1.

Figure 2a shows the UV–vis and PL characteristics of the green QDs used in this report with the extremely narrow emission bandwidth of the QDs [full width at half-maximum (fwhm) of ~30 nm]. The QY of QD was estimated to be ~63%. The diameter of a QD was 10 nm, as indicated in the TEM image (Figure 2b).

Panels a and b of Figure 3 illustrate the EL characteristics of QD-LEDs with various hole materials, including polymer (poly-TPD and PVK) and small molecules (CBP and TPD), and a summary of QD-LED performances for the various hole transport materials is given in Table 2. The luminance and current efficiency values of the QD-LED devices based on small molecules are much lower than those of the devices based on polymer materials. These results are attributed to the low packing densities of the small molecule thin films.²² Therefore, small molecules are not suitable for HTLs of high-quality QD-LED applications in spite of their high hole mobilities and low HOMO levels.

The QD-LED based on PVK showed values of maximal luminescence and current efficiency >2 times higher than those of the device based on poly-TPD. These results are attributed to the lower HOMO energy level of PVK (−5.8 eV) compared to that of poly-TPD (−5.2 eV) in spite of its hole mobility being lower than that of poly-TPD (Table 1). This result indicates that the HOMO level of HTL plays a more important

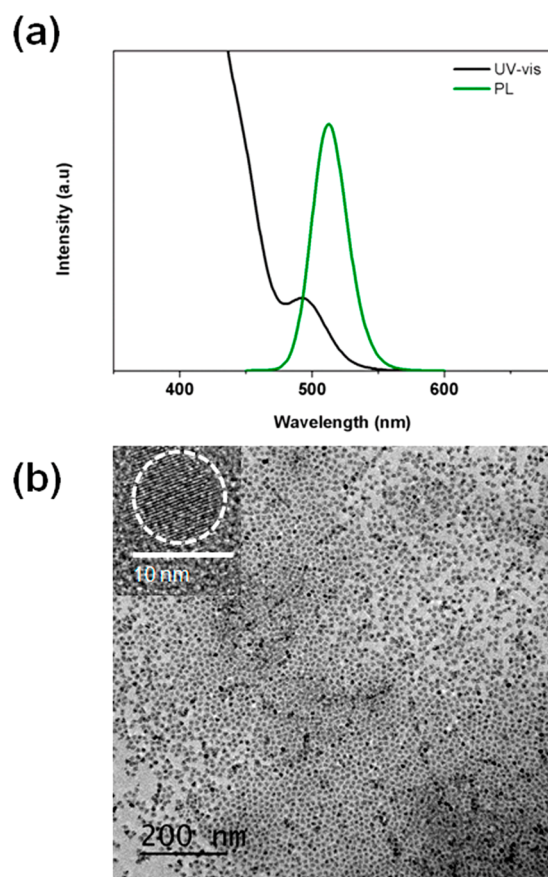


Figure 2. (a) UV-vis and PL spectra of QDs. (b) TEM image of QDs (inset, a high-resolution TEM image of a single QD).

role than mobility in the performance of QD-LEDs. Hence, PVK was selected as the hole transport material to improve device performances in this work.

3.2. Small Molecule Added PVK as HTL for QD-LEDs.

Even though our best results were obtained with the PVK polymer as the HTL, hole mobility was limited to $2.5 \times 10^{-6} \text{ cm}^2 \text{ V}^{-1} \text{ s}^{-1}$,²³ resulting in the high turn-on voltage and low current density of the devices due to the imbalance of hole-electron injection during device operation (Figure 3a). To overcome these drawbacks, different concentrations of TCTA, CBP, or TPD small molecules were added to the PVK layer to increase the hole mobility of the HTL.

Figure 4 shows the effect of addition of up to 40 wt % TCTA to PVK on the EL characteristics of QD-LEDs. The decreased turn-on voltage and increased current density indicate that the hole injection was improved by adding TCTA (5–40 wt %). The current efficiency of QD-LEDs was considerably enhanced up to 27% at 20 wt % TCTA (Figure 4c and Table 3). However, further addition of TCTA (30–40 wt %) decreased the current efficiency considerably. Upon addition of 40 wt % TCTA, the current efficiency was reduced to a level even lower than that of a PVK-only device possibly because of the problem of thin film formation observed in small molecule-only devices. The EL spectra of QD-LED and the correlation between the current efficiency and luminance of devices versus TCTA fraction are plotted in panels c and d of Figure 4. As can be seen, upon addition of 5–10 wt % TCTA, even though the enhanced luminance can be obtained, the current efficiency is decreased. The increase in brightness and current

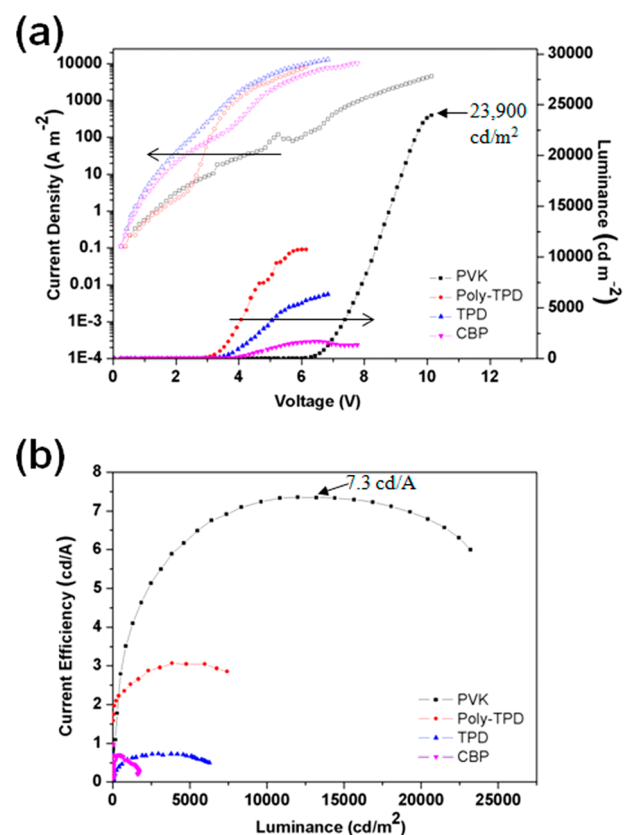


Figure 3. (a) Current (I), voltage (V), and luminance (L) characteristics and (b) current efficiency of QD-LEDs based on different hole transport materials.

Table 2. Summary of Device Performances for Different Hole Transport Materials

hole transport materials	turn-on voltage ^a (V)	maximal luminescence (cd/m ²)	current efficiency (cd/A)
PVK	6.5	23900	7.3
poly-TPD	3.0	10700	3.0
TPD	3.5	6300	0.7
CBP	4.0	1800	0.6

^aDefined as the applied voltage when the luminance is detected by the luminance meter.

Table 3. Summary of Device Performances for HTLs of PVK-only and PVK with TCTA

HTL	turn-on voltage (V)	maximal luminescence (cd/m ²)	current efficiency (cd/A)
PVK-only	7.2	30000	11.0
PVK with TCTA (5 wt %)	5.8	38000	9.5
PVK with TCTA (10 wt %)	5.6	38000	9.0
PVK with TCTA (20 wt %)	5.5	40900	14.0
PVK with TCTA (30 wt %)	5.5	44000	12.0
PVK with TCTA (40 wt %)	5.0	39500	10.0

efficiency is shown obviously with a higher doping concentration (20–30 wt %).

Additions of CBP and TPD to PVK were also investigated. However, both CBP and TPD have rather low glass transition temperatures (T_g values of ~ 62 and ~ 65 °C, respectively), while the glass transition temperature of TCTA is much higher (~ 151 °C).²⁴ Consequently, the CBP or TPD dopant was

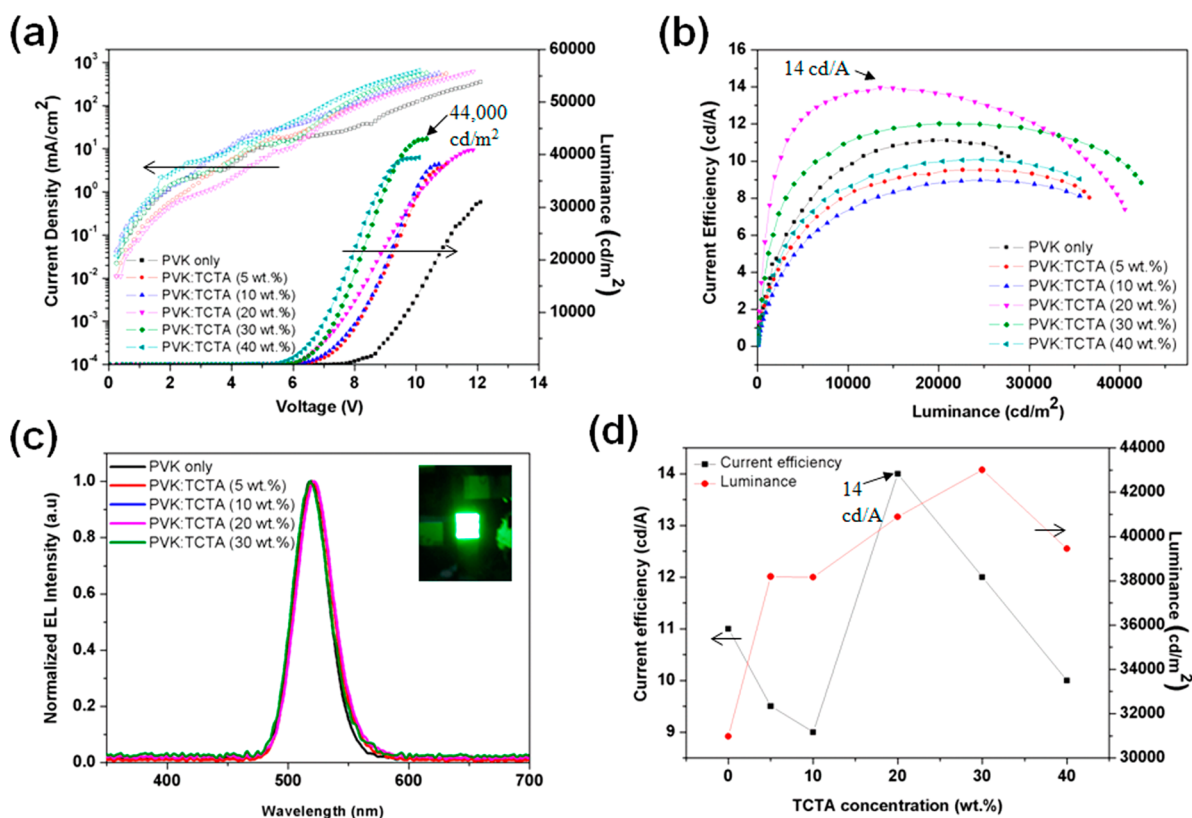


Figure 4. (a) Current (I), voltage (V), and luminance (L) characteristics and (b) current efficiency of QD-LEDs based on PVK-only and PVK-doped TCTA (5–40 wt %). (c) Normalized EL spectra of QD-LEDs for different TCTA concentrations (inset, photograph of a QD-LED with a pixel size of 3.0 mm \times 3.0 mm). (d) Current efficiency and luminance of QD-LEDs vs TCTA concentration.

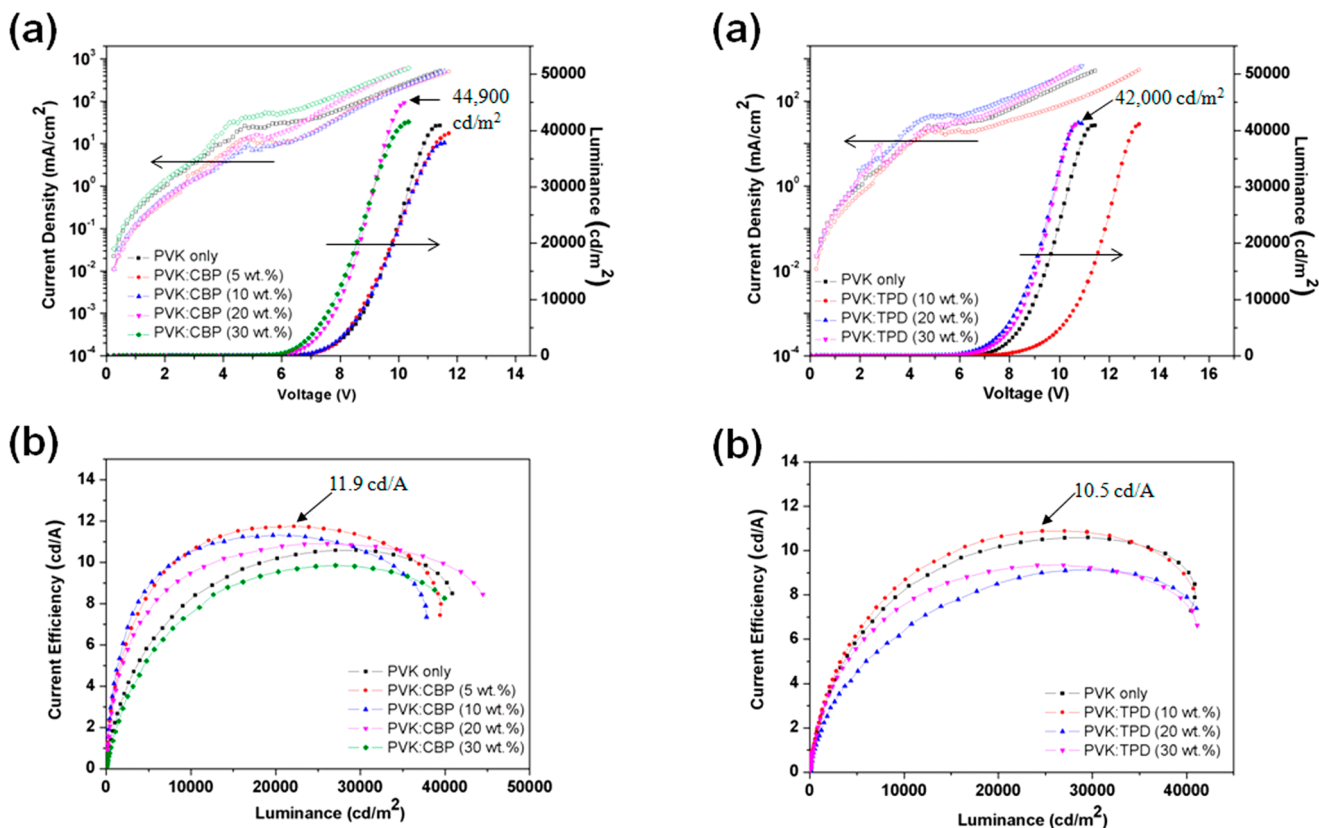


Figure 5. (a) Current (I), voltage (V), and luminance (L) characteristics and (b) current efficiency of QD-LEDs based on PVK-only and PVK-doped CBP (5–30 wt %).

Figure 6. (a) Current (I), voltage (V), and luminance (L) characteristics and (b) current efficiency of QD-LEDs based on PVK-only and PVK-doped TPD (10–30 wt %).

easily crystallized,^{24,25} resulting in limited improvement in device performance. As shown in Figures 5a and 6a, upon addition of both 20 and 30 wt % TPD and CBP, the current density increased and the turn-on voltage decreased and addition of CBP provided enhanced luminance; however, the improved brightness was not obtained upon addition of TPD. More importantly, the current efficiency was enhanced considerably by utilizing CBP as a dopant; meanwhile, a slight increase was seen in the case of a QD-LED based on the TPD dopant (Figures 5b and 6b). These results can be explained by the lower HOMO level of CBP (−6.0 eV) compared to that of TPD (−5.4 eV) at similar hole mobilities of CBP and TPD (Table 1).

4. CONCLUSION

We investigated the effects of different hole transport materials on the performance of QD-LEDs. PVK was found to be a good polymer material for the HTL because of its low HOMO level. The low HOMO level of the hole transport material was a dominating factor affecting QD-LED device performance. The hole mobilities of HTLs were considerably improved upon addition of small molecule TCTA, CBP, or TPD. The CBP and TPD dopants had some negative effects on device performance because of their rather low T_g values. Addition of TCTA, however, with a relatively high T_g , effectively improved the EL performance of QD-LEDs. At a doping concentration of 20 wt %, the maximal current efficiency of the QD-LED was increased by >27%. In addition, the lower turn-on voltage, the higher current density, and the higher luminance could be achieved upon addition of TCTA. We successfully demonstrated a QD-LED device with a maximal brightness of 40900 cd/m², a peak current efficiency of 14.0 cd/A, and a narrow fwhm (<35 nm).

AUTHOR INFORMATION

Corresponding Author

*E-mail: hchae@skku.edu. Telephone: +82-31-290-7263. Fax: +82-31-290-7272.

Notes

The authors declare no competing financial interest.

ACKNOWLEDGMENTS

This research was supported by the Basic Science Research Program through the National Research Foundation of Korea (NRF) funded by the Ministry of Education, Science and Technology (2011-0006268). This research was also supported by the MKE (The Ministry of Knowledge Economy), Korea, under the ITRC (Information Technology Research Center) support program (NIPA-2012-H0301-12-4013) supervised by the NIPA (National IT Industry Promotion Agency).

REFERENCES

- (1) Reiss, P.; Protière, M.; Li, L. *Small* **2009**, *5*, 154–168.
- (2) Shen, H.; Wang, S.; Wang, H.; Niu, J.; Qian, L.; Yang, Y.; Titov, A.; Hyvonen, J.; Zheng, Y.; Li, L. S. *ACS Appl. Mater. Interfaces* **2013**, *5*, 4260–4265.
- (3) He, S.; Li, S.; Wang, F.; Wang, A. Y.; Lin, J.; Tan, Z. *Nanotechnology* **2013**, *24*, 175–201.
- (4) Li, J. J.; Wang, Y. A.; Guo, W.; Keay, J. C.; Mishima, T. D.; Johnson, M. B.; Peng, X. *J. Am. Chem. Soc.* **2003**, *125*, 12567–12575.
- (5) Reiss, P.; Bleuse, J.; Pron, A. *Nano Lett.* **2002**, *2*, 781–784.
- (6) Wood, V.; Bulović, V. *Nano Rev.* **2010**, *1*, S202.
- (7) Wood, V.; Panzer, M. J.; Halpert, J. E.; Caruge, J.-M.; Bawendi, M. G.; Bulović, V. *ACS Nano* **2009**, *3*, 3581–3586.

- (8) Caruge, J. M.; Halpert, J. E.; Wood, V.; Bulović, V.; Bawendi, M. G. *Nat. Photonics* **2008**, *2*, 247–250.
- (9) Cho, K.-S.; Lee, E. K.; Joo, W.-J.; Jang, E.; Kim, T.-H.; Lee, S. J.; Kwon, S.-J.; Han, J. Y.; Kim, B.-K.; Choi, B. L.; Kim, J. M. *Nat. Photonics* **2009**, *3*, 341–345.
- (10) Qian, L.; Zheng, Y.; Xue, J.; Holloway, P. H. *Nat. Photonics* **2011**, *5*, 543–548.
- (11) Kwak, J.; Bae, W. K.; Lee, D.; Park, I.; Lim, J.; Park, M.; Cho, H.; Woo, H.; Yoon, D. Y.; Char, K.; Lee, S.; Lee, C. *Nano Lett.* **2012**, *12*, 2362–2366.
- (12) Caruge, J.-M.; Halpert, J. E.; Bulović, V.; Bawendi, M. G. *Nano Lett.* **2006**, *6*, 2991–2994.
- (13) Coe-Sullivan, S.; Steckel, J. S.; Woo, W.-K.; Bawendi, M. G.; Bulović, V. *Adv. Mater.* **2005**, *15*, 1117–1124.
- (14) Niu, Y.-H.; Munro, A. M.; Cheng, Y.-J.; Tian, Y.; Liu, M. S.; Zhao, J.; Bardecker, J. A.; Plante, I. J.-L.; Ginger, D. S.; Jen, A. K.-Y. *Adv. Mater.* **2007**, *19*, 3371–3376.
- (15) Zhao, J.; Bardecker, J. A.; Munro, A. M.; Liu, M. S.; Niu, Y.; Ding, I.-K.; Luo, J.; Chen, B.; Jen, A. K.-Y.; Ginger, D. S. *Nano Lett.* **2006**, *6*, 463–467.
- (16) Bae, W. K.; Kwak, J.; Park, J. W.; Char, K.; Lee, C.; Lee, S. *Adv. Mater.* **2009**, *21*, 1690–1694.
- (17) Lakowicz, J. R. *Principles of Fluorescence Spectroscopy*, 3rd ed.; Springer: New York, 2006.
- (18) Demas, J. N.; Crosby, G. A. *J. Phys. Chem.* **1971**, *75*, 991–1024.
- (19) Leck, K. S.; Divayana, Y.; Zhao, D.; Xuyong, Y.; Abiyasa, A. P.; Mutlugun, E.; Yuan, G.; Shuwei, L.; Swee, T. T.; Xiao, W. S.; Demir, H. V. *ACS Appl. Mater. Interfaces* **2013**, *5*, 6535–6540.
- (20) Yang, X.; Mutlugun, E.; Zhao, Y.; Gao, Y.; Leck, K. S.; Ma, Y.; Ke, L.; Tan, S. T.; Demir, H. V.; Sun, X. W. *Small* **2013**, DOI:10.1002/sml.201301199.
- (21) Stouwdam, J. W.; Janssen, R. A. J. *J. Mater. Chem.* **2008**, *18*, 1889–1894.
- (22) Duan, L.; Hou, L.; Lee, T.-W.; Qiao, J.; Zhang, D.; Dong, G.; Wang, L.; Qiu, Y. *J. Mater. Chem.* **2010**, *20*, 6392–6407.
- (23) Lee, D.-H.; Liu, Y.-P.; Lee, K.-H.; Chae, H.; Cho, S. M. *Org. Electron.* **2010**, *11*, 427–433.
- (24) Tao, Y.; Yang, C.; Qin, J. *Chem. Soc. Rev.* **2011**, *40*, 2943–2970.
- (25) Zhang, T.; Liang, Y.; Cheng, J.; Li, J. *J. Mater. Chem. C* **2013**, *1*, 757–764.
- (26) Thesen, M. W.; Höfer, B.; Debeaux, M.; Janietz, S.; Wedel, A.; Köhler, A.; Johannes, H.-H.; Krueger, H. J. *Polym. Sci., Part A: Polym. Chem.* **2010**, *48*, 3417–3430.